

Self-Supervised Audio-Visual Representation Learning with Relaxed Cross-Modal Synchronicity

Pritam Sarkar^{1,2} and Ali Etemad¹

¹ Queen’s University, Canada

² Vector Institute

{pritam.sarkar, ali.etemad}@queensu.ca

<https://pritamqu.github.io/CrissCross>

Abstract. We present **CrissCross**, a self-supervised framework for learning audio-visual representations. A novel notion is introduced in our framework whereby in addition to learning the intra-modal and standard ‘synchronous’ cross-modal relations, CrissCross also learns ‘asynchronous’ cross-modal relationships. We show that by relaxing the temporal synchronicity between the audio and visual modalities, the network learns strong generalized representations. Our experiments show that strong augmentations for both audio and visual modalities with relaxation of cross-modal temporal synchronicity optimize performance. To pretrain our proposed framework, we use 3 different datasets with varying sizes, Kinetics-Sound, Kinetics400, and AudioSet. The learned representations are evaluated on a number of downstream tasks namely action recognition, sound classification, and retrieval. CrissCross shows state-of-the-art performances on action recognition (UCF101 and HMDB51) and sound classification (ESC50 and DCASE). The codes and pretrained models will be made publicly available.

1 Introduction

In recent years, self-supervised learning has shown great promise in learning strong representations without human-annotated labels [11, 12, 9], and emerged as a strong competitor for fully-supervised pretraining. There are a number of benefits to such methods. Firstly, they reduce the time and resources required for expensive human-annotations and allow researchers to directly use large uncurated datasets for learning meaningful representations. Moreover, the models trained in a self-supervised fashion learn more abstract representations, which can be useful in solving a variety of downstream tasks without needing to train the models from scratch.

Given the abundance of videos, their spatio-temporal information-rich nature, and the fact that in most cases they contain both audio and visual streams, self-supervised approaches are strong alternatives to fully-supervised methods for video representation learning. Moreover, the high dimensionality and multi-modal nature of videos makes them difficult to annotate, further motivating the use of self-supervision.

The common and standard practice in self-supervised audio-visual representations learning is to learn intra-modal and synchronous cross-modal relationships between the audio and visual streams. In this regard, existing solutions try to learn audio-visual representations by maintaining a tight temporal synchronicity between the two modalities [2, 27, 3, 5]. Yet, the impact of learning temporally asynchronous cross-modal relationships in the context of self-supervised learning has not been explored. This notion deserves deeper exploration as learning such temporally asynchronous cross-modal relationships may in fact result in increased invariance and distinctiveness in the learned representations.

In this study, in an attempt to explore the notion mentioned above, we present **CrissCross** a novel framework to learn robust generalized representations from videos (a simple illustration is presented in Figure 1). In addition to learning intra-modal and standard synchronous cross-modal relations, CrissCross introduces a novel concept to learn cross-modal representations through *relaxing* time-synchronicity between corresponding audio and visual segments. We refer to this as ‘asynchronous cross-modal’ optimization, a concept that has not been explored in prior works. We use 3 datasets of different sizes: Kinetics-Sound [4], Kinetics400 [23], and AudioSet [16], to pretrain CrissCross. We evaluate CrissCross on different downstream tasks, namely action recognition, sound classification, and retrieval. We use 2 popular benchmarks UCF101 [58] and HMDB51 [28] to perform action recognition and retrieval, while ESC50 [47] and DCASE[59] are used for sound classification.

Contributions. The key contributions of this work are as follows:

- We present a novel framework for multi-modal self-supervised learning by relaxing the audio-visual temporal synchronicity to learn effective generalized representations. Our method is simple, data efficient, and less resource intensive, yet learns robust multi-modal representations for a variety of downstream tasks.
- We perform an in-depth study to explore the performance of the proposed framework and its major concepts. Additionally we extensively investigate a wide range of audio-visual augmentation techniques capable of learning strong audio-visual representations within our framework.
- Comparing the performance of our method to prior works, CrissCross achieves state-of-the-arts on UCF101 [58], HMDB [28], ESC50 [47], and DCASE[59] when pretrained on Kinetics400 [23]. Moreover, when trained with AudioSet [16], CrissCross achieves better or competitive performances versus the current state-of-the-arts.

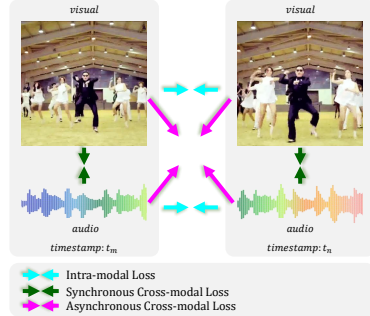


Fig. 1: **Overview.** CrissCross learns effective audio-visual representations by exploiting not only intra-modal, but also synchronous and *asynchronous* cross-modal relations. The sample frames are obtained from Kinetics400[23].

- Lastly, when pretrained on the small-scale dataset Kinetics-Sound [4], Criss-Cross outperforms fully-supervised pretraining [33] by 1.4% and 7.4%, as well as prior self-supervised state-of-the-art [33] by 11.1% and 19.9% on UCF101 and HMDB51 respectively. To the best of our knowledge, very few prior works have attempted to pretrain on such small datasets, and in fact this is the first time where self-supervised pretraining outperforms full supervision on action recognition in this setup.

We hope our proposed self-supervised method can motivate researchers to further explore the notion of *asynchronous* multi-modal representation learning.

2 Related Work

2.1 Self-supervised Learning

Self-supervised learning aims to learn generalized representations of data without any human annotated labels through properly designed pseudo tasks (also known as pretext tasks). Self-supervised learning has recently drawn significant attention in different fields of deep learning such as image [11,12,38,10,18,9,52], video [41,40,3,5,45,2,37], and wearable data [55,54,56] analysis among others.

In self-supervised learning, the main focus of interest lies in designing novel pseudo-tasks to learn useful representations. We briefly mention some of the popular categories in the context of self-supervised video representation learning, namely, *i*) context-based, *ii*) generation-based, *iii*) clustering-based, and *iv*) contrastive learning-based. Various pretext tasks have been proposed in the literature exploring the spatio-temporal context of video frames, for example, temporal order prediction [29], puzzle solving [25,39,1], rotation prediction [22], and others. Generation-based video feature learning methods refer to the process of learning feature representations through video generation [66,64,53], video colorization [62], and frame or clip prediction [34,51,6,30,15], among a few others. Clustering-based approaches [3,5] rely on self-labeling where data is fed to the network and the extracted feature embeddings are clustered using a classical clustering algorithm such as k-means, followed by using the cluster assignments as the pseudo-labels for training the neural network. The key concept of contrastive learning [12,38,18,10,41,45] is that in the embedding space, ‘positive’ samples should be similar to each other, and ‘negative’ samples should have discriminative properties. Using this concept, several prior works [41,40,45,33] have attempted to learn representations by minimizing the distance between positive pairs and maximizing the distance between negative pairs.

2.2 Audio-Visual Representation Learning

Typically in multi-modal self-supervised learning, multiple networks are jointly trained on the same pretext tasks towards maximizing the mutual information between multiple data streams [3,41,27,68,67,24,57]. Following, we briefly discuss some of the prior works [27,3,41,33] on audio-visual multi-modal representation learning. A multi-modal self-supervised task introduced in AVTS [27], leveraging the natural synergy between audio-visual data. The network is trained to distinguish whether the given audio and visual sequences are ‘in sync’ or ‘out of sync’. The authors propose a two-stream network, where one stream receives

audio as input and the other network is fed with the visual data. Next, audio and visual embeddings are fused at the end of the convolution layers, and the joint representations are used to minimize the contrastive loss. In XDC [3], the authors introduce a framework to learn cross-modal representations through a self-labelling process. In XDC, cluster assignments obtained from the audio-visual representations are used as pseudo-labels to train the backbones. Specifically, the pseudo-labels computed from audio embeddings are used to train the visual backbone, while the pseudo-labels computed using visual embeddings are used to train the audio network. A self-supervised learning framework based on contrastive learning is proposed in AVID [41], to learn audio-visual representations from video. AVID performs instance discrimination as the pretext task. AVID [41] redefines the notion of positive and negative pairs based on their similarity and dissimilarity in the feature space, followed by optimizing a noise contrastive estimator loss to learn multi-modal representations. This is different from AVTS [27], where audio-visual segments originated from the same samples are considered as positive pairs, and segments originated from different samples are considered as negative pairs.

Distinctions to our work. We acknowledge that earlier works [27, 41, 33] show great promise in learning strong multimodal representations. However, we identify some limitations in prior work, which we attempt to address in our study. Most earlier works based on contrastive learning try to find negative and positive pairs through a complex process. Moreover, we notice that over time, the definition of ‘positive’ and ‘negative’ pairs have been changing. For instance, we find distinct differences in such definitions amongst some earlier works [27, 41, 40]. In this study, our goal is to propose a simple yet effective solution for learning multi-modal representations. Additionally, we would like to highlight that earlier works [41, 5, 3, 33] use massive distributed GPU setups (40-64 GPUs), which are significant bottlenecks when computing resources are limited. In this study, we effectively train our method on only 4-8 GPUs. Lastly, as discussed earlier, we hypothesize that to learn effective generalized features, the synchronicity between audio and visual segments could be relaxed. Interestingly, it may appear that our approach is in contrast to some prior works that suggest synchronization [27, 50] is helpful in learning strong multi-modal representations. Nonetheless, our framework exploits both synchronous and asynchronous cross-modal relationships in an attempt to learn both time-dependant and time-invariant representations.

3 Method

Here we present the core concepts of our proposed framework. First, we briefly discuss the uni-modal concepts that our model is built on, which are adopted from an earlier work, SimSiam [12]. Next, we introduce the multi-modal concepts of our framework to jointly learn self-supervised audio-visual representations.

3.1 Uni-modal Learning

To separately learn visual and audio representations, we follow the setup proposed in [12], which we briefly mention here for the sake of completeness. Let’s, assume an encoder f , where f is composed of a convolutional backbone followed

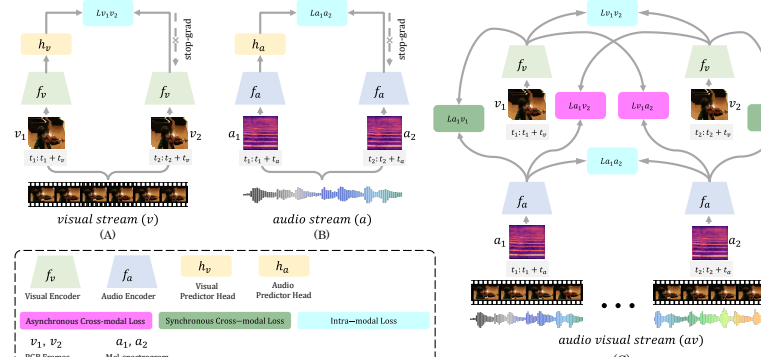


Fig. 2: **Our proposed framework.** We present the uni-modal baselines and the multi-modal setup. The uni-modal setups (Visual-only and Audio-only) are presented in (A) and (B) respectively. The multi-modal framework, CrissCross, is presented in (C). In case of uni-modal setups, we show the predictor heads, as well as the stop-grad to elaborate on the frameworks. However, in case of CrissCross, we skip those components for the sake of simplicity.

by an MLP projection head, and an MLP prediction head h . Two augmented views of a sample x are created as x_1 and x_2 . Accordingly, the objective is to minimize the symmetrized loss:

$$\mathcal{L}_{x_1, x_2} = \frac{1}{2}\mathcal{D}(p_1, \mathbf{S}(z_2)) + \frac{1}{2}\mathcal{D}(p_2, \mathbf{S}(z_1)), \quad (1)$$

where \mathcal{D} denotes the negative cosine similarity, and output vectors p_1 and z_2 are computed as $h(f(x_1))$ and $f(x_2)$ respectively. Similarly, p_2 and z_1 are computed as $h(f(x_2))$ and $f(x_1)$ respectively. Further, we apply stop-grad on the latent vector z_1 and z_2 , which is denoted by \mathbf{S} . We extend this concept to learn visual and audio representations as discussed below.

To learn visual representations from videos, we use a visual encoder f_v and a predictor head h_v . We generate two augmented views of a sample v as v_1 and v_2 , where v_1 belongs to timestamp t_1 , and v_2 belongs to timestamp t_2 . Finally, we optimize the loss \mathcal{L}_{v_1, v_2} using Equation 1. We present this concept in Figure 2A. Similarly we generate two augmented views of an audio sample a as a_1 and a_2 , where a_1 and a_2 belong to timestamps t_1 and t_2 respectively. We use a_1 and a_2 to optimize \mathcal{L}_{a_1, a_2} (following Equation 1) using an audio encoder f_a and a predictor head h_a to learn audio representations. A pictorial representation of this method is depicted in Figure 2B.

3.2 Multi-modal Learning

Here, we discuss the multi-modal learning components of our proposed framework. We present different ways to learn multi-modal representations, namely Intra-modal, Synchronous Cross-modal, Asynchronous Cross-modal, and finally, CrissCross, which blends all three previous methods. We explain each of these concepts below.

Intra-modal Representations. To learn multi-modal representations, our first approach is a joint representation learning method where we train the visual

and audio networks with a common objective function \mathcal{L}_{intra} . Here, \mathcal{L}_{intra} is calculated as $(\mathcal{L}_{v_1, v_2} + \mathcal{L}_{a_1, a_2})/2$, where \mathcal{L}_{v_1, v_2} and \mathcal{L}_{a_1, a_2} are uni-modal losses for visual and audio learning as discussed earlier.

Synchronous Cross-modal Representations. To learn cross-modal audio-visual representations, we calculate the distance between the two different modalities, particularly by calculating \mathcal{L}_{a_1, v_1} corresponding to a_1 , v_1 , and \mathcal{L}_{a_2, v_2} , corresponding to a_2 , v_2 . Finally, we optimize the synchronous cross-modal loss \mathcal{L}_{sync} , which is calculated as $(\mathcal{L}_{a_1, v_1} + \mathcal{L}_{a_2, v_2})/2$.

Asynchronous Cross-modal Representations. Next, we introduce an *asynchronous* (or cross-time) cross-modal loss to learn local time-invariant representations. Here, we attempt to optimize *asynchronous* cross-modal representations by calculating \mathcal{L}_{a_1, v_2} to minimize the distance between feature vectors corresponding to a_1 and v_2 . Similarly, we calculate \mathcal{L}_{a_2, v_1} to minimize the distance between feature vectors corresponding to a_2 and v_1 . Finally, we calculate the asynchronous cross-modal loss \mathcal{L}_{async} as $(\mathcal{L}_{a_1, v_2} + \mathcal{L}_{a_2, v_1})/2$.

CrissCross. Our proposed multi-modal representation learning method is named CrissCross. In this setup, we combine the objective functions of Intra-modal, Synchronous Cross-modal, and Asynchronous Cross-modal learning. Accordingly, we define the final objective function $\mathcal{L}_{CrissCross}$ as $(\mathcal{L}_{intra} + \mathcal{L}_{sync} + \mathcal{L}_{async})/3$, which gives:

$$\mathcal{L}_{CrissCross} = \frac{1}{6}(\mathcal{L}_{a_1, a_2} + \mathcal{L}_{v_1, v_2} + \mathcal{L}_{a_1, v_1} + \mathcal{L}_{a_2, v_2} + \mathcal{L}_{a_1, v_2} + \mathcal{L}_{a_2, v_1}). \quad (2)$$

We present the proposed CrissCross framework in Figure 2C and its pseudocode in Section S2.

3.3 Relaxing Time Synchronicity

Audio and visual modalities from the same source clip generally maintain a very strong correlation, which makes them suitable for multi-modal representation learning as one modality can be used as a supervisory signal for the other in a self-supervised setup. However, our intuition behind CrissCross is that these cross-modal temporal correlations do not necessarily need to follow a strict frame-wise coupling. Instead, we hypothesize that relaxing cross-modal temporal synchronicity to some extent can help in learning more generalized representations.

To facilitate this idea within CrissCross, we present 5 different temporal sampling methods to create the augmented views of a source clip. These 5 **temporal sampling methods** are designed to explore varying amounts of **temporal synchronicity** when learning cross-modal relationships. (i) *Same-timestamp*: where both the audio and visual segments are sampled from the exact same time window (denoted as *none* in terms of temporal relaxation). (ii) *Overlapped*: where the two views of the audio-visual segments share 50% overlap amongst them (denoted as *mild* relaxation). (iii) *Adjacent*: where adjacent frame sequences and audio segments are sampled (denoted as *medium* relaxation). (iv) *Far-apart*: in which we sample one view from the first half of the source clip, while the other view is sampled from the second half of the source clip (denoted as *extreme* relaxation). (v) *Random*: where the two audio-visual segments are sampled in a temporally random manner (denoted as *mixed* relaxation). It should

be noted that the concept of relaxing cross-modal time synchronicity doesn't apply to the uni-modal setups.

4 Experiment

The details of the experiment setup and the findings of our thorough empirical studies for investigating the major concepts of our proposed framework are presented here.

4.1 Experiment Setup

Datasets. We use 3 datasets of different sizes for pretraining purposes, namely, Kinetics-Sound [4], Kinetics400 [23], and AudioSet [16]. Following the standard practices of prior works [41,40,2,3,5,27], we evaluate our self-supervised methods on two types of downstream tasks, (*i*) action recognition using UCF101 [58] and HMDB51 [28], and (*ii*) sound classification using ESC50 [47] and DCASE[59]. We provide additional details for all the datasets in Section S3.

Architectures. Following the standard practice among prior works [41,40,3,5,45] we use R(2+1)D [63] and ResNet [21] as the visual and audio backbones. We use a slightly modified version [41] of R(2+1)D-18 [63] as the backbone for visual feature extraction. To extract the audio features, we use ResNet-18 [21]. The projector and predictor heads of the self-supervised framework are composed of MLPs. The details of all of the architectures are presented in Section S6.

Pretraining Details. To train the network in a self-supervised fashion with audio-visual inputs, we downsample the visual streams to 16 frames per second, and feed 0.5-second frame sequences to the visual encoder. We resize the spatial resolution to 112^2 , so the final input dimension to the visual encoder becomes $3 \times 8 \times 112^2$, where 3 represents the 3 channels of RGB. Next, we downsample the audio signals to 16kHz, and segment them into 2-second segments. Next, we transform the segmented raw audio waveforms to mel-spectrograms using 80 mel filters, we set the hop size as 10 milliseconds, and FFT window length as 1024. Finally, we feed spectrograms of shape 80×200 to the audio encoder. We use Adam [26] optimizer with a cosine learning rate scheduler [31] to pretrain the encoders and use a fixed learning rate to train the predictors. We provide additional details of the hyperparameters in Section S7.

4.2 Empirical Study

Here we present the empirical study performed to investigate the major concepts of our proposed framework. During the empirical study all of the models are trained using Kinetics-Sound [4] for 100 epochs, unless stated otherwise. We perform transfer learning to evaluate visual and audio representations. Linear evaluation is performed using a one-vs-all SVM classifier (linear kernel) on the fixed features to quickly evaluate our models on downstream tasks. We prefer one-vs-all SVM over training an FC layer to limit parameter tuning at this point. Moreover, to limit memory overhead, we use 0.5 seconds (8 frames) of visual input and 2 seconds of audio input to extract the fixed features. The details of the linear evaluation protocol is mentioned in Section S5. We use UCF101 to evaluate visual representations on action recognition, and ESC50 to evaluate

Table 1: **Ablation study.** We present the results of CrissCross and its uni-modal and multi-modal ablation variants. The differences between the ablated variants and CrissCross are also presented in red.

#	Method	Pretrain Db.	Downstream Db.	
			UCF101	ESC50
(a)	\mathcal{L}_{v_1, v_2}	Kinetics-Sound	69.1($\downarrow 5.7$)	-
(b)	\mathcal{L}_{a_1, a_2}	Kinetics-Sound	-	62.0($\downarrow 17.0$)
(c)	\mathcal{L}_{intra}	Kinetics-Sound	69.7($\downarrow 5.1$)	71.8($\downarrow 7.2$)
(d)	\mathcal{L}_{sync}	Kinetics-Sound	70.1($\downarrow 4.7$)	75.8($\downarrow 3.2$)
(e)	\mathcal{L}_{async}	Kinetics-Sound	69.1($\downarrow 5.7$)	74.8($\downarrow 4.2$)
(f)	$\mathcal{L}_{sync} + \mathcal{L}_{intra}$	Kinetics-Sound	73.8($\downarrow 1.0$)	78.0($\downarrow 1.0$)
(g)	$\mathcal{L}_{async} + \mathcal{L}_{intra}$	Kinetics-Sound	72.4($\downarrow 2.4$)	75.3($\downarrow 3.7$)
(h)	$\mathcal{L}_{async} + \mathcal{L}_{sync}$	Kinetics-Sound	69.1($\downarrow 5.7$)	74.8($\downarrow 4.2$)
(i)	$\mathcal{L}_{CrissCross}$	Kinetics-Sound	74.8	79.0
(j)	$\mathcal{L}_{sync} + \mathcal{L}_{intra}$	Kinetics400	75.8($\downarrow 4.1$)	78.5($\downarrow 3.5$)
(k)	$\mathcal{L}_{async} + \mathcal{L}_{intra}$	Kinetics400	74.9($\downarrow 5.0$)	76.3($\downarrow 5.7$)
(l)	$\mathcal{L}_{CrissCross}$	Kinetics400	79.9	82.0

audio representation on sound classification. All of our empirical studies are evaluated using split-1 of both the datasets.

4.2.1 Ablation Study

We present the ablation results in Table 1 to show the improvement made by optimizing intra-modal, synchronous cross-modal, and asynchronous cross-modal losses. To illustrate the benefits of learning asynchronous relations, we perform ablation studies on 2 pretraining datasets, Kinetics-Sound[4] and Kinetics400[23]. First, using Kinetics-Sound, we train the framework in uni-modal setups, denoted as \mathcal{L}_{v_1, v_2} and \mathcal{L}_{a_1, a_2} . We report the top-1 accuracy of UCF101 and ESC50 as 69.1% and 62.0% respectively. Next, we train the network in a multi-modal setup, where we find that \mathcal{L}_{sync} outperforms the other multi-modal variants with single-term losses (\mathcal{L}_{intra} and \mathcal{L}_{async}) as well as uni-modal baselines (\mathcal{L}_{v_1, v_2} and \mathcal{L}_{a_1, a_2}). Further study shows that combining different multi-modal losses improve the model performance. Specifically, we notice that $\mathcal{L}_{CrissCross}$ outperforms \mathcal{L}_{sync} by 4.7% and 3.2% on action recognition and sound classification, respectively.

We further investigate the benefits of $\mathcal{L}_{CrissCross}$ versus the top 2 ablation competitors ($\mathcal{L}_{sync} + \mathcal{L}_{intra}$ and $\mathcal{L}_{async} + \mathcal{L}_{intra}$) on the large and diverse Kinetics400 [23]. We observe that $\mathcal{L}_{CrissCross}$ outperforms these variants by **4.1%** and **3.5%** in action recognition and sound classification, respectively, showing the significance of asynchronous cross-modal optimization in a multi-modal setup. Our intuition is that as Kinetics-Sound consists of a few hand-picked classes that are prominently manifested in both audio and visual modalities, the performance gain of CrissCross is less prominent. However, Kinetics400 is considerably larger in scale and is comprised of highly diverse action classes. It therefore benefits more from the more generalized representations learned by asynchronous cross-modal optimization.

Table 2: **Temporal sampling.** Exploring temporal sampling methods for multi-modal and uni-modal representation learning.

Temp. Sampling (Temp. Relaxation)	Uni-modal		CrissCross	
	UCF101	ESC50	UCF101	ESC50
Same (None)	55.6	62.0	73.2	77.0
Overlapped (Mild)	68.3	62.0	73.9	79.0
Adjacent (Medium)	68.1	58.8	71.5	77.8
Random (Random)	65.1	60.3	72.5	77.8
Far-apart (Extreme)	63.8	58.3	72.8	78.5

Table 3: **Augmentations.** Exploring audio-visual augmentations.

Uni	Visual	UCF101	Audio	ESC50
	MSC-HF-CJ	62.3	VJ	44.8
	MSC-HF-CJ-GS	68.1	VJ-M	49.5
	MSC-HF-CJ-GS-C	68.3	VJ-M-TW	49.5
	MSC-HF-CJ-GS-GB	68.7	VJ-M-RC	62.0
	MSC-HF-CJ-GS-GB-C	69.1		
Multi	Visual + Audio	UCF101	ESC50	
	MSC-HF-CJ-GS-C + VJ-M-RC	73.9	79.0	
	MSC-HF-CJ-GS-GB + VJ-M-RC	73.5	79.0	
	MSC-HF-CJ-GS-GB-C + VJ-M-RC	74.8	79.0	

4.2.2 Understanding Relaxed Time-synchronicity

In this subsection we study how different amounts of temporal relaxation in cross-modal synchronicity impacts CrissCross. To do so, we exploit 5 different temporal sampling methods as discussed earlier in Section 3. We further aim to identify the best temporal sampling method in a uni-modal setup. We train Visual-only, Audio-only, and CrissCross frameworks using different temporal sampling methods. The results presented in Table 2 show that the *overlapped* sampling method works the best overall for both the uni-modal setups. The *same* temporal sampling method shows poor performance on the visual-only model. However, it performs as good as the *overlapped* sampling method on the audio-only model. Interestingly, the *far-apart* sampling shows the worst performance amongst other methods on the Audio-only model, whereas, the Visual-only model works reasonably well with the *far-apart* sampling method. Next, we test these 5 temporal sampling methods on CrissCross and present the results in Table 2.

Interestingly, we notice that the *same* and *far-apart* methods, which work poorly in the uni-modal setups, perform reasonably well in a multi-modal setup. We believe, the improvement of performance here is because of the strong supervision received from the other modality. Nonetheless, we find that the *overlapped* temporal sampling method (*mild* temporal relaxation) performs relatively better, outperforming the other approaches.

4.2.3 Exploring Audio-Visual Augmentations

We perform an in-depth study to explore the impact of different audio and visual augmentations.

Visual Augmentations. We explore a wide range of visual augmentations. As a starting point, we adopt the basic spatial augmentations used in [41], which consists of Multi-Scale Crop (MSC), Horizontal Flip (HF), and Color Jitter (CJ). Additionally, we explore other augmentations, namely Gray Scale (GS), Gaussian Blur (GB) [11], and Cutout (C) [14], which show great performance in image-based self-supervised learning [11,65]. We explore almost all the possible combinations of different visual augmentations in a uni-modal setup and present the results in Table 3. The results show that strong augmentations improve the top-1 accuracy by 6.8% in comparison to basic augmentations used in [41]. We mention the augmentation parameters and implementation details in Section S4.

Temporal Consistency of Spatial Augmentations. While investigating different spatial augmentations, we are also interested to know if the spatial aug-

mentations should be consistent at the frame level or whether they should be random (i.e., vary among consecutive frames within a sequence). We refer to these concepts as *temporally consistent* or *temporally random*. We perform an experiment where we apply MSC-HF-CJ-GS randomly at the frame level, and compare the results to applying the same augmentations consistently across all the frames of a sequence. Our results show that maintaining temporal consistency in spatial augmentations across consecutive frames is beneficial, which is in line with the findings in [49]. Specifically, *Temporally random* augmentations, results in top-1 accuracy of 53.69%, whereas, the same augmentations applied in a *temporally consistent* manner results in 68.09%.

Audio Augmentations. Similar to visual augmentations, we thoroughly investigate a variety of audio augmentations. Our audio augmentations include, Volume Jitter (VJ), Time and Frequency Masking (Mask) [43], Random Crop (RC) [42], and Time Warping (TW) [43]. We also explore almost all the possible combinations of these augmentations, and present the results in Table 3. Our findings show that time-frequency masking and random crop improve the top-1 accuracy by 17.25% compared to the base variant. We also notice that time warping doesn't improve the performance and is also quite computationally expensive. Hence, going forward we do not use time warping during pretraining. We present the augmentation parameters and additional implementation details in Section S4.

Audio-Visual Augmentations. We conduct further experiments on a few combinations of augmentations in a *multi-modal* setup. We pick the top performing augmentations obtained from the uni-modal variants and apply them concurrently. The results are presented in Table 3 where we find that the results are consistent with the uni-modal setups, as the combination of MSC-HF-CJ-GS-GB-C and VJ-M-RC performs the best in comparison to the other combinations.

4.2.4 Exploring Design Choices

Predictor. Our empirical study shows that the predictor head plays an important role to effectively train the audio and visual encoders to learn good representations. The predictor architecture is similar to [12]. For the sake of completeness, we provide the details of the predictor head in Section S6. We explore (i) different learning rates, and (ii) using a common vs. a separate predictor in the multi-modal setup. It should be noted that none of the variants cause a collapse, even-though we notice considerable differences in performance. We present the findings in the following paragraphs. Additionally, the training curves of both experiments are presented in Section S1.

Similar to [12], we use a constant learning rate for the predictors. However, unlike [12], where the predictor learning rate is the same as the base learning rate of the encoder, we find that a higher predictor learning rate helps the network to learn better representations in both uni-modal and multi-modal setups. In case of CrissCross, setting the predictor learning rate to be the same as the base learning rate results in unstable training, and the loss curve shows oscillating behavior. We empirically find that setting the predictor learning rate to 10 times the base learning rate, works well. We present the results in Table 4.

Table 4: A comparative study of different predictor lr w.r.t the base lr (lr_b).

	UCF101		ESC50	
	lr_b	$10 \times lr_b$	lr_b	$10 \times lr_b$
\mathcal{L}_{a_1, a_2}	-	-	60.3	62.0
\mathcal{L}_{v_1, v_2}	66.0	69.1	-	-
$\mathcal{L}_{CrissCross}$	59.0	74.8	62.3	79.0

Table 5: Exploring design choices for the predictor and projector heads.

	Predictor		Projector	
	Common	Separate	2 Layers	3 Layers
UCF101	73.6	74.8	72.4	74.8
ESC50	75.3	79.0	75.0	79.0

Table 6: We present the results of linear evaluation on action recognition and sound classification.

Pretraining Dataset	Size	HMDB51	UCF101	Kinetics400	ESC50	DCASE
Kinetics-Sound	22K	45.7	78.1	39.0	82.8	93.0
Kinetics400	240K	50.0	83.9	44.5	86.8	96.0
AudioSet	1.8M	56.2	87.7	49.4	90.5	97.0

Next, we evaluate whether the framework can be trained in a multi-modal setup with a common predictor head instead of separate predictor heads (default setup). In simple terms, one predictor head would work towards identity mapping for both audio and video feature vectors. To test this, l2-normalized feature vectors $f_v(v)$ and $f_a(a)$ are fed to the predictor, which are then used in a usual manner to optimize the cost function. The results are presented in Table 5. We observe that though such a setup works somewhat well, having separate predictors is beneficial for learning better representations.

Projector. We present a comparative study of projection heads with 2 layers vs. 3 layers. We notice 2.4% and 4% improvements in top-1 accuracies when using 3 layers instead of 2 on action recognition and sound classification respectively (please see Table 5). Note that we use 3 fully-connected layers as the default setup for the projectors. The architecture details are presented in Section S6.

4.3 Linear Evaluation

To evaluate the quality of the representations learned through pretraining, we perform linear evaluation on action recognition (HMDB51, UCF101, and Kinetics400) and sound classification (ESC50 and DCASE). As mentioned earlier, we use 3 different sized datasets, i.e., Kinetics-Sound, Kinetics400, and AudioSet for pretraining. In Table 6 we report the top-1 accuracies averaged over all the splits. We provide the details of the evaluation protocol in Section S5. We notice a steady improvement in performance as the dataset size increases, which shows CrissCross can further be scaled on even larger datasets like IG65M [17]. To evaluate CrissCross in a more critical setting, we test the downstream task performance on Kinetics400 while pretrained with the small-scale Kinetics-Sound (10% of Kinetics400). Our results show CrissCross performs reasonably well even in such a difficult setting, achieving a top-1 accuracy of 39.0%.

5 Comparison to the State-of-the-Arts

We compare the proposed CrissCross framework against the state-of-the-arts methods. We validate visual representations on action recognition, and audio representations on sound classification. We present the details in the following.

Table 7: **SOTA comparison on action recognition.** Top-1 accuracy averaged over all the splits on UCF101 and HMDB51 are presented. We group the results based on the pretraining dataset. Additionally, we present the architecture details and finetuning input size of the respective methods.

Method	Pretrain Dataset	Compute	Backbone	Finetune Resolution	UCF101	HMDB51
Fully Supervised[33]	KS	-	3D-ResNet18	32×224^2	86.9	53.1
CM-ACC[33]	KS	40 GPUs	3D-ResNet18	32×224^2	77.2	40.6
CrissCross	KS	4 GPUs	R(2+1)D-18	32×224^2	88.3	60.5
Fully Supervised[45]	K400	-	R(2+1)D-18	32×224^2	95.0	74.0
XDC [3]	K400	64 GPUs	R(2+1)D-18	8×224^2	74.2	39.0
AVID [41]	K400	64 GPUs	R(2+1)D-18	8×224^2	83.7	49.5
Robust-xID [40]	K400	8 GPUs	R(2+1)D-18	8×224^2	81.9	49.5
CrissCross	K400	8 GPUs	R(2+1)D-18	8×224^2	86.9	54.3
DPC [19]	K400	4 GPUs	S3D	25×128^2	75.7	35.7
CBT [60]	K400	8 GPUs	S3D	16×112^2	79.5	44.6
AVTS [27]	K400	4 GPUs	MC3-18	25×224^2	84.1	52.5
SeLaVi [5]	K400	64 GPUs	R(2+1)D-18	32×112^2	83.1	47.1
XDC [3]	K400	64 GPUs	R(2+1)D-18	32×224^2	86.8	52.6
AVID [41]	K400	64 GPUs	R(2+1)D-18	32×224^2	87.5	60.8
GDT [48]	K400	64 GPUs	R(2+1)D-18	32×224^2	90.9	62.3
Robust-xID [40]	K400	8 GPUs	R(2+1)D-18	32×224^2	85.6	55.0
CMAC [37]	K400	8 GPUs	R(2+1)D-18	32×224^2	90.3	61.1
CM-ACC [33]	K700*	40 GPUs	3D-ResNet18	32×224^2	90.2	61.8
CM-ACC [33]	AS*	40 GPUs	3D-ResNet18	32×224^2	90.7	62.3
CrissCross	K400	8 GPUs	R(2+1)D-18	32×224^2	91.5	64.7
Fully Supervised[50]	AS	-	R(2+1)D-18	32×224^2	96.8	75.9
XDC [3]	AS	64 GPUs	R(2+1)D-18	8×224^2	84.9	48.8
AVID [41]	AS	64 GPUs	R(2+1)D-18	8×224^2	88.6	57.6
CrissCross	AS	8 GPUs	R(2+1)D-18	8×224^2	89.4	58.3
AVTS [27]	AS	4 GPUs	MC3-18	25×224^2	87.7	57.3
XDC [3]	AS	64 GPUs	R(2+1)D-18	32×224^2	93.0	63.7
AVID [41]	AS	64 GPUs	R(2+1)D-18	32×224^2	91.5	64.7
MMV [2]	AS	32 TPUs	R(2+1)D-18	32×224^2	91.5	70.1
BraVe [30]	AS	16 TPUs	R(2+1)D-18	32×224^2	94.1	71.1
CM-ACC [33]	AS	40 GPUs	R(2+1)D-18	32×224^2	93.5	67.2
CrissCross	AS	8 GPUs	R(2+1)D-18	32×224^2	92.4	66.8

Note: K700* and AS* refer to 240K samples from K700 and AS respectively.

5.1 Action Recognition

Full-Finetuning. In line with [3,5,41,45,33], we benchmark CrissCross using UCF101 [58] and HMDB51 [28] on action recognition. We briefly mention the experimental setup for downstream evaluation here and redirect readers to Section S5 for additional information. We use the pretrained 18-layer R(2+1)D [63] as the video backbone, and fully finetune it on action recognition. We use the Kinetics-Sound [4], Kinetics400 [23], and AudioSet [16] for pretraining. For a fair comparison to earlier works, we adopt 2 setups for finetuning, once with 8 frames, and the other with 32 frames. In both these setups, we use a spatial resolution of 224^2 . We tune the model using the split-1 of both datasets and report the top-1 accuracy averaged over all the splits. We notice large variability in experimental setups in the literature in terms of different backbones (e.g., deeper convnets, transformer-based architectures, etc.) [48,49,46], pretraining inputs (e.g., the addition of optical flow or text to audio-visual data, etc.) [48,49,2], and pretraining datasets, making it impractical to compare to all the prior

works. Following the inclusion criteria of earlier works [45,3,41,40], we compare CrissCross with methods that use similar backbones, inputs, and pretraining datasets.

The comparison of CrissCross with recent works is presented in Table 7. The fully-supervised baselines compared to CrissCross are taken directly from prior works [37,45,50,3] and have not been implemented by ourselves. When pretrained with Kinetics400, CrissCross achieves state-of-the-arts on UCF101 and HMDB51 in both the fine-tuning setups. CrissCross outperforms current state-of-the-arts AVID [41] on UCF101 and HMDB51 by 3.2% and 4.8%, respectively, when fine-tuned with 8 frame inputs. Additionally, while fine-tuned with 32 frames, CrissCross outperforms current state-of-the-arts GDT [45] by 0.6% and 2.4% on UCF101 and HMDB51 respectively.

Next, CrissCross outperforms the current state-of-the-art AVID [41], when pretrained on AudioSet and fine-tuned with 8-frame inputs, on both UCF101 and HMDB51. When fine-tuned with 32-frame inputs, CrissCross achieves competitive results amongst the leading methods. We note that some of the prior works show slightly better performance compared to ours in some settings. We conjecture this to be due to the use of higher spatio-temporal resolution inputs in these models. E.g., BraVe [50] is trained with 2 views of 32×112^2 and 128×112^2 , and the input size for MMV [2] and CM-ACC [33] are 32×224^2 and 16×224^2 , respectively. In comparison, CrissCross is pretrained with visual inputs of size 8×112^2 . However, we expect the performance of our model to improve further by using such higher resolutions, given the trend shown in [61,50].

In addition to the commonly used Kinetics400 and AudioSet, we further evaluate CrissCross while pretrained on the small-scale Kinetics-Sound [4]. Here, we observe significant improvements compared to CM-ACC [33] on UCF101 (88.3 vs. 77.2) and HMDB51 (60.5 vs. 40.6). Additionally, CrissCross outperforms fully-supervised pretraining by 1.4% and 7.4% on UCF101 and HMDB51 respectively when both the fully-supervised and self-supervised methods are pretrained on Kinetics-Sound [4]. To the best of our knowledge, this is the first time that self-supervision outperforms full-supervised pretraining on action recognition using the same small-scale dataset, showing that our method performs well on limited pretraining data.

Retrieval. In addition to full finetuning, we also compare the performance of CrissCross in an unsupervised setup. Following prior works [40,45,5], we perform a retrieval experiment. We use the split-1 of both UCF101 [58] and HMDB51 [28] and present the comparison with prior works in Table 8. We observe that CrissCross outperforms the current state-of-the-arts on UCF101, while achieving competitive results for HMDB51. We present additional details for the retrieval experiment setup in Section S5.

5.2 Sound Classification

To evaluate audio representations learned by CrissCross, we use two popular benchmarks ESC50 [47] and DCASE [59] to perform sound classification. We find large variability of experimental setups in the literature for evaluating audio representations. For instance, different backbones, input lengths, datasets, and

Table 8: **SOTA comparison on action retrieval.** We present the accuracy of video retrieval on UCF and HMDB datasets for different numbers of nearest neighbors, using the video backbone pretrained on Kinetics400.

Method	UCF			HMDB		
	R@1	R@5	R@20	R@1	R@5	R@20
ST Order [8]	25.7	36.2	49.2	-	-	-
SpeedNet [7]	13.0	28.1	49.5	-	-	-
Clip Order [68]	14.1	30.3	51.1	7.6	22.9	48.8
VCP [32]	18.6	33.6	53.5	7.6	24.4	53.6
VSP [13]	24.6	41.9	76.9	10.3	26.6	54.6
CoCLR [20]	55.9	70.8	82.5	26.1	45.8	69.7
SeLaVi [5]	52.0	68.6	84.5	24.8	47.6	75.5
GDT [45]	57.4	73.4	88.1	25.4	51.4	75.0
Robust-xID [40]	60.9	79.4	90.8	30.8	55.8	79.7
CrissCross	63.8	78.7	89.9	26.4	50.5	77.7

Table 9: **SOTA comparison on sound classification.** Top-1 accuracies averaged over all the splits on ESC50 and DCASE are presented. Additionally, the linear evaluation input size for ESC50 and architecture of the respective methods are presented. K400 and AS refer to Kinetics400 and AudioSet respectively.

Method	Backbone	ESC50			DCASE		
		sec.	KS	K400	AS	KS	K400
AVTS [27]	VGG-8	2	-	76.7	80.6	-	91.93
XDC [3]	ResNet-18	2	-	78.0	84.8	-	91.95
AVID [11]	ConvNet-9	2	-	79.1	89.1	-	93.96
MMV [2]	ResNet-50	5	-	-	85.6	-	-
BraVe [50]	ResNet-50	5	-	-	90.4	-	-
CrissCross	ResNet-18	2	79.5	81.5	86.7	93	96
CrissCross	ResNet-18	5	82.8	86.8	90.5		

evaluation protocols (linear evaluation, full-finetuning) have been used, making it impractical to compare to all the prior works. Following [41, 27, 3, 50, 2], we perform linear evaluation on ESC50 [47] and DCASE [59]. To be able to compare our work to a larger number of prior works, we perform linear evaluation using both 2 and 5-second inputs for ESC50, and 1-second input for DCASE. Please refer to Section S5 for additional details on the evaluation protocols. As presented in Table 9, when pretrained on Kinetics400 and evaluated with 2-second inputs, CrissCross outperforms the current state-of-the-art AVID [41] by 2.4%. Additionally, when pretrained on AudioSet and evaluated with 5-second inputs, CrissCross marginally outperforms the current state-of-the-art, BraVe [50]. Finally, CrissCross sets new state-of-the-art by outperforming all prior works on DCASE when pretrained on Kinetics400 and AudioSet.

6 Summary

We propose a novel self-supervised framework to learn audio-visual representations by considering intra-modal, as well as, synchronous and *asynchronous* cross-modal relationships. We conduct a thorough study investigating the major concepts of our framework. Our findings show that properly composed strong augmentations and relaxation of cross-modal temporal synchronicity is beneficial for learning effective audio-visual representations. These representations can then be used for a variety of downstream tasks including action recognition, sound classification, and retrieval.

Limitations. The notion of asynchronous cross-modal optimization has not been explored beyond audio-visual modalities. For example, our model can be expanded to consider more than 2 modalities (e.g., audio, visual, and text), which are yet to be studied. Additionally, we notice a considerable performance gap between full-supervision and self-supervision when both methods are pretrained with the same large-scale dataset (Kinetics400 or AudioSet), showing room for further improvement.

Acknowledgment

We are grateful to Bank of Montreal and Mitacs for funding this research. We are thankful to Vector Institute and SciNet HPC Consortium for helping with the computation resources.

References

1. Ahsan, U., Madhok, R., Essa, I.: Video jigsaw: Unsupervised learning of spatiotemporal context for video action recognition. In: WACV. pp. 179–189 (2019) [3](#)
2. Alayrac, J.B., Recasens, A., Schneider, R., Arandjelovic, R., Ramapuram, J., De Fauw, J., Smaira, L., Dieleman, S., Zisserman, A.: Self-supervised multimodal versatile networks. NeurIPS **2**(6), 7 (2020) [2](#), [3](#), [7](#), [12](#), [13](#), [14](#), [21](#), [23](#)
3. Alwassel, H., Mahajan, D., Korbar, B., Torresani, L., Ghanem, B., Tran, D.: Self-supervised learning by cross-modal audio-video clustering. NeurIPS **33** (2020) [2](#), [3](#), [4](#), [7](#), [12](#), [13](#), [14](#), [21](#), [23](#), [24](#)
4. Arandjelovic, R., Zisserman, A.: Look, listen and learn. In: ICCV. pp. 609–617 (2017) [2](#), [3](#), [7](#), [8](#), [12](#), [13](#), [21](#), [27](#)
5. Asano, Y.M., Patrick, M., Rupprecht, C., Vedaldi, A.: Labelling unlabelled videos from scratch with multi-modal self-supervision. In: NeurIPS (2020) [2](#), [3](#), [4](#), [7](#), [12](#), [13](#), [14](#), [21](#), [24](#)
6. Babaeizadeh, M., Finn, C., Erhan, D., Campbell, R.H., Levine, S.: Stochastic variational video prediction. In: ICLR (2018) [3](#)
7. Benaim, S., Ephrat, A., Lang, O., Mosseri, I., Freeman, W.T., Rubinstein, M., Irani, M., Dekel, T.: Speednet: Learning the speediness in videos. In: CVPR. pp. 9922–9931 (2020) [14](#)
8. Buchler, U., Brattoli, B., Ommer, B.: Improving spatiotemporal self-supervision by deep reinforcement learning. In: ECCV (2018) [14](#)
9. Caron, M., Bojanowski, P., Joulin, A., Douze, M.: Deep clustering for unsupervised learning of visual features. In: ECCV. pp. 132–149 (2018) [1](#), [3](#)
10. Caron, M., Misra, I., Mairal, J., Goyal, P., Bojanowski, P., Joulin, A.: Unsupervised learning of visual features by contrasting cluster assignments. In: NeurIPS (2020) [3](#)
11. Chen, T., Kornblith, S., Norouzi, M., Hinton, G.: A simple framework for contrastive learning of visual representations. In: ICML. pp. 1597–1607 (2020) [1](#), [3](#), [9](#), [21](#)
12. Chen, X., He, K.: Exploring simple siamese representation learning. In: CVPR. pp. 15750–15758 (2021) [1](#), [3](#), [4](#), [10](#), [25](#), [26](#)
13. Cho, H., Kim, T., Chang, H.J., Hwang, W.: Self-supervised spatio-temporal representation learning using variable playback speed prediction. arXiv preprint arXiv:2003.02692 (2020) [14](#)
14. DeVries, T., Taylor, G.W.: Improved regularization of convolutional neural networks with cutout. arXiv preprint arXiv:1708.04552 (2017) [9](#)
15. Finn, C., Goodfellow, I., Levine, S.: Unsupervised learning for physical interaction through video prediction. NeurIPS **29**, 64–72 (2016) [3](#)
16. Gemmeke, J.F., Ellis, D.P., Freedman, D., Jansen, A., Lawrence, W., Moore, R.C., Plakal, M., Ritter, M.: Audio set: An ontology and human-labeled dataset for audio events. In: ICASSP. pp. 776–780 (2017) [2](#), [7](#), [12](#), [21](#)
17. Ghadiyaram, D., Tran, D., Mahajan, D.: Large-scale weakly-supervised pre-training for video action recognition. In: CVPR. pp. 12038–12047 (2019) [11](#)
18. Grill, J.B., Strub, F., Altché, F., Tallec, C., Richemond, P., Buchatskaya, E., Doersch, C., Pires, B., Guo, Z., Azar, M., et al.: Bootstrap your own latent: A new approach to self-supervised learning. In: NeurIPS (2020) [3](#)

19. Han, T., Xie, W., Zisserman, A.: Video representation learning by dense predictive coding. In: CVPRW. pp. 0–0 (2019) [12](#)
20. Han, T., Xie, W., Zisserman, A.: Self-supervised co-training for video representation learning. In: NeurIPS (2020) [14](#)
21. He, K., Zhang, X., Ren, S., Sun, J.: Deep residual learning for image recognition. In: CVPR. pp. 770–778 (2016) [7](#), [24](#)
22. Jing, L., Yang, X., Liu, J., Tian, Y.: Self-supervised spatiotemporal feature learning via video rotation prediction. arXiv preprint arXiv:1811.11387 (2018) [3](#)
23. Kay, W., Carreira, J., Simonyan, K., Zhang, B., Hillier, C., Vijayanarasimhan, S., Viola, F., Green, T., Back, T., Natsev, P., et al.: The kinetics human action video dataset. arXiv preprint arXiv:1705.06950 (2017) [2](#), [7](#), [8](#), [12](#), [21](#), [23](#), [27](#)
24. Khare, A., Parthasarathy, S., Sundaram, S.: Self-supervised learning with cross-modal transformers for emotion recognition. In: SLT. pp. 381–388 (2021) [3](#)
25. Kim, D., Cho, D., Kweon, I.S.: Self-supervised video representation learning with space-time cubic puzzles. In: AAAI. vol. 33, pp. 8545–8552 (2019) [3](#)
26. Kingma, D.P., Ba, J.: Adam: A method for stochastic optimization. In: ICLR (2015) [7](#), [25](#)
27. Korbar, B., Tran, D., Torresani, L.: Cooperative learning of audio and video models from self-supervised synchronization. In: NeurIPS. pp. 7774–7785 (2018) [2](#), [3](#), [4](#), [7](#), [12](#), [14](#), [21](#)
28. Kuehne, H., Jhuang, H., Garrote, E., Poggio, T., Serre, T.: Hmdb: a large video database for human motion recognition. In: ICCV. pp. 2556–2563 (2011) [2](#), [7](#), [12](#), [13](#), [21](#), [24](#)
29. Lee, H.Y., Huang, J.B., Singh, M., Yang, M.H.: Unsupervised representation learning by sorting sequences. In: CVPR (2017) [3](#)
30. Liang, X., Lee, L., Dai, W., Xing, E.P.: Dual motion gan for future-flow embedded video prediction. In: ICCV. pp. 1744–1752 (2017) [3](#)
31. Loshchilov, I., Hutter, F.: Sgdr: Stochastic gradient descent with warm restarts. In: ICLR (2017) [7](#)
32. Luo, D., Liu, C., Zhou, Y., Yang, D., Ma, C., Ye, Q., Wang, W.: Video cloze procedure for self-supervised spatio-temporal learning. In: AAAI (2020) [14](#)
33. Ma, S., Zeng, Z., McDuff, D., Song, Y.: Active contrastive learning of audio-visual video representations. In: ICLR (2020) [3](#), [4](#), [12](#), [13](#)
34. Mathieu, M., Couprie, C., LeCun, Y.: Deep multi-scale video prediction beyond mean square error. In: ICLR (2016) [3](#)
35. McFee, B., Raffel, C., Liang, D., Ellis, D.P., McVicar, M., Battenberg, E., Nieto, O.: librosa: Audio and music signal analysis in python. In: Python in Science Conference. vol. 8, pp. 18–25 (2015) [22](#)
36. Micikevicius, P., Narang, S., Alben, J., Diamos, G., Elsen, E., Garcia, D., Ginsburg, B., Houston, M., Kuchaiev, O., Venkatesh, G., et al.: Mixed precision training. In: ICLR (2018) [26](#)
37. Min, S., Dai, Q., Xie, H., Gan, C., Zhang, Y., Wang, J.: Cross-modal attention consistency for video-audio unsupervised learning. arXiv preprint arXiv:2106.06939 (2021) [3](#), [12](#), [13](#)
38. Misra, I., Maaten, L.v.d.: Self-supervised learning of pretext-invariant representations. In: CVPR. pp. 6707–6717 (2020) [3](#)
39. Misra, I., Zitnick, C.L., Hebert, M.: Shuffle and learn: unsupervised learning using temporal order verification. In: ECCV. pp. 527–544 (2016) [3](#)
40. Morgado, P., Misra, I., Vasconcelos, N.: Robust audio-visual instance discrimination. In: CVPR. pp. 12934–12945 (2021) [3](#), [4](#), [7](#), [12](#), [13](#), [14](#), [21](#), [24](#)

41. Morgado, P., Vasconcelos, N., Misra, I.: Audio-visual instance discrimination with cross-modal agreement. In: CVPR. pp. 12475–12486 (2021) [3](#), [4](#), [7](#), [9](#), [12](#), [13](#), [14](#), [21](#), [23](#), [24](#)
42. Niizumi, D., Takeuchi, D., Ohishi, Y., Harada, N., Kashino, K.: Byol for audio: Self-supervised learning for general-purpose audio representation. arXiv preprint arXiv:2103.06695 (2021) [10](#), [22](#)
43. Park, D.S., Chan, W., Zhang, Y., Chiu, C.C., Zoph, B., Cubuk, E.D., Le, Q.V.: SpecAugment: A simple data augmentation method for automatic speech recognition. arXiv preprint arXiv:1904.08779 (2019) [10](#), [22](#)
44. Paszke, A., Gross, S., Massa, F., Lerer, A., Bradbury, J., Chanan, G., Killeen, T., Lin, Z., Gimelshein, N., Antiga, L., et al.: Pytorch: An imperative style, high-performance deep learning library. NeurIPS **32**, 8026–8037 (2019) [21](#), [26](#)
45. Patrick, M., Asano, Y.M., Kuznetsova, P., Fong, R., Henriques, J.F., Zweig, G., Vedaldi, A.: On compositions of transformations in contrastive self-supervised learning. In: Proceedings of the IEEE/CVF International Conference on Computer Vision. pp. 9577–9587 (2021) [3](#), [7](#), [12](#), [13](#), [14](#), [23](#), [24](#)
46. Patrick, M., Huang, P.Y., Misra, I., Metze, F., Vedaldi, A., Asano, Y.M., Henriques, J.F.: Space-time crop & attend: Improving cross-modal video representation learning. In: ICCV. pp. 10560–10572 (2021) [12](#)
47. Piczak, K.J.: ESC: Dataset for Environmental Sound Classification. In: ACM Conference on Multimedia. pp. 1015–1018. (2015) [2](#), [7](#), [13](#), [14](#), [21](#)
48. Piergiovanni, A., Angelova, A., Ryoo, M.S.: Evolving losses for unsupervised video representation learning. In: CVPR. pp. 133–142 (2020) [12](#)
49. Qian, R., Meng, T., Gong, B., Yang, M.H., Wang, H., Belongie, S., Cui, Y.: Spatiotemporal contrastive video representation learning. In: CVPR. pp. 6964–6974 (2021) [10](#), [12](#)
50. Recasens, A., Luc, P., Alayrac, J.B., Wang, L., Strub, F., Tallec, C., Malinowski, M., Patraucean, V., Altché, F., Valko, M., et al.: Broaden your views for self-supervised video learning. arXiv preprint arXiv:2103.16559 (2021) [4](#), [12](#), [13](#), [14](#), [23](#)
51. Reda, F.A., Liu, G., Shih, K.J., Kirby, R., Barker, J., Tarjan, D., Tao, A., Catanzaro, B.: Sdc-net: Video prediction using spatially-displaced convolution. In: ECCV. pp. 718–733 (2018) [3](#)
52. Roy, S., Etemad, A.: Self-supervised contrastive learning of multi-view facial expressions. In: ICMI. pp. 253–257 (2021) [3](#)
53. Saito, M., Matsumoto, E., Saito, S.: Temporal generative adversarial nets with singular value clipping. In: ICCV. pp. 2830–2839 (2017) [3](#)
54. Sarkar, P., Etemad, A.: Self-supervised ecg representation learning for emotion recognition. IEEE Transactions on Affective Computing (2020) [3](#)
55. Sarkar, P., Etemad, A.: Self-supervised learning for ecg-based emotion recognition. In: ICASSP. pp. 3217–3221 (2020) [3](#)
56. Sarkar, P., Lobmaier, S., Fabre, B., Berg, G., Mueller, A., Frasch, M.G., Antonelli, M.C., Etemad, A.: Detection of maternal and fetal stress from ecg with self-supervised representation learning. arXiv e-prints pp. arXiv–2011 (2020) [3](#)
57. Siriwardhana, S., Kaluarachchi, T., Billinghurst, M., Nanayakkara, S.: Multimodal emotion recognition with transformer-based self supervised feature fusion. IEEE Access **8**, 176274–176285 (2020) [3](#)
58. Soomro, K., Zamir, A.R., Shah, M.: Ucf101: A dataset of 101 human actions classes from videos in the wild. arXiv preprint arXiv:1212.0402 (2012) [2](#), [7](#), [12](#), [13](#), [21](#), [24](#)
59. Stowell, D., Giannoulis, D., Benetos, E., Lagrange, M., Plumbley, M.D.: Detection and classification of acoustic scenes and events. IEEE Transactions on Multimedia **17**(10), 1733–1746 (2015) [2](#), [7](#), [13](#), [14](#), [21](#)

60. Sun, C., Baradel, F., Murphy, K., Schmid, C.: Learning video representations using contrastive bidirectional transformer. arXiv preprint arXiv:1906.05743 (2019) [12](#)
61. Touvron, H., Vedaldi, A., Douze, M., Jégou, H.: Fixing the train-test resolution discrepancy. NeurIPS **32** (2019) [13](#)
62. Tran, D., Bourdev, L., Fergus, R., Torresani, L., Paluri, M.: Deep end2end voxel2voxel prediction. In: CVPRW. pp. 17–24 (2016) [3](#)
63. Tran, D., Wang, H., Torresani, L., Ray, J., LeCun, Y., Paluri, M.: A closer look at spatiotemporal convolutions for action recognition. In: CVPR. pp. 6450–6459 (2018) [7, 12, 24](#)
64. Tulyakov, S., Liu, M.Y., Yang, X., Kautz, J.: MoCoGAN: Decomposing motion and content for video generation. In: CVPR. pp. 1526–1535 (2018) [3](#)
65. Van Gansbeke, W., Vandenhende, S., Georgoulis, S., Proesmans, M., Van Gool, L.: Scan: Learning to classify images without labels. In: ECCV. pp. 268–285 (2020) [9](#)
66. Vondrick, C., Pirsavash, H., Torralba, A.: Generating videos with scene dynamics. NeurIPS **29**, 613–621 (2016) [3](#)
67. Wang, J., Jiao, J., Bao, L., He, S., Liu, W., Liu, Y.H.: Self-supervised video representation learning by uncovering spatio-temporal statistics. PAMI (2021) [3](#)
68. Xu, D., Xiao, J., Zhao, Z., Shao, J., Xie, D., Zhuang, Y.: Self-supervised spatiotemporal learning via video clip order prediction. In: CVPR. pp. 10334–10343 (2019) [3, 14, 24](#)
69. You, Y., Gitman, I., Ginsburg, B.: Large batch training of convolutional networks. arXiv preprint arXiv:1708.03888 (2017) [25](#)

Supplementary Material

The organization of the supplementary material is as follows:

- Section **S1**: Training Statistics
- Section **S2**: Pseudocode;
- Section **S3**: Details of all the datasets;
- Section **S4**: Details of data augmentations;
- Section **S5**: Downstream evaluation protocols;
- Section **S6**: Architecture details;
- Section **S7**: Hyperparameters and training details;
- Section **S8**: Qualitative analysis.
- Section **S9**: Broader Impact.

S1 Training Statistics

To provide a better understanding of our training process, we present the loss curves of the self-supervised pretraining. In Figures **S1** and **S2** we present the training curves obtained during design choice explorations on Kinetics-Sound. Figure **S1** shows that, setting the predictor learning rate to be the same as the base learning rate, results in oscillating behavior at the initial phase of the pretraining, which results in learning poor representations as already discussed in the main paper. Next, we notice that using the common predictor head, results in the training losses saturating very quickly ultimately yielding worse performance compared to the use of separate predictor heads. Additionally, when analysing the training curves in the default setup, the intra-modal losses reach a steady state quite early in comparison to the cross-modal losses. The total loss still decreases beyond our scheduled training iterations. However, we stop the training when no improvement is noticed in the downstream tasks.

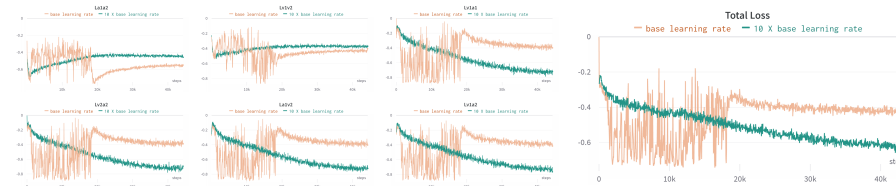


Fig. S1: We present the loss curves for different predictor learning rates. **La1a2** and **Lv1v2** refer to the intra-modal losses; **La1v1** and **La2v2** denote the synchronous cross-modal losses; and finally **La1v2** and **Lv1a2** refer to the asynchronous cross-modal losses. Note that the minimum possible value for each loss is -1.

S2 Pseudocode

We present the pseudocode of our proposed CrissCross framework in Algorithm **1**. Please note this pseudocode is written in a Pytorch-like format.

Algorithm 1 CrissCross pseudocode (PyTorch-like)

```

class CrissCross(nn.Module):
    def __init__(fv, fa, hv, ha):
        super().__init__()
        """Initialize CrissCross Module
        Args:
            fv: visual encoder (backbone+projection mlp)
            fa: audio encoder (backbone+projection mlp)
            hv: visual predictor (prediction mlp)
            ha: audio predictor (prediction mlp)
        Returns:
            CrissCross Module
        """

    def forward(v1, v2, a1, a2):
        """Forward function CrissCross Module
        Args:
            v1, v2: minibatch of augmented visual samples
            a1, a2: minibatch of augmented audio samples
        Returns:
            L_CrissCross: total loss
        """

        # visual
        zv1, zv2 = fv(v1), fv(v2) # visual embeddings
        pv1, pv2 = hv(zv1), hv(zv2) # predictor output

        # audio
        za1, za2 = fa(a1), fa(a2) # audio embeddings
        pa1, pa2 = ha(za1), ha(za2) # predictor output

        # loss calculation,
        # D: loss function
        # D: loss function

        # asynchronous cross-modal loss
        Lv1a2 = D(pv1, za2)/2 + D(pa2, zv1)/2 # v1-a2
        La1v2 = D(pa1, zv2)/2 + D(pv2, za1)/2 # a1-v2
        L_async = (Lv1a2 + La1v2)/2

        # synchronous cross-modal loss
        Lv1a1 = D(pv1, za1)/2 + D(pa1, zv1)/2 # v1-a1
        Lv2a2 = D(pv2, za2)/2 + D(pa2, zv2)/2 # v2-a2
        L_sync = (Lv1a1 + Lv2a2)/2

        # intra-modal loss
        Lv1v2 = D(pv1, zv2)/2 + D(pv2, zv1)/2 # v1-v2
        La1a2 = D(pa1, za2)/2 + D(pa2, za1)/2 # a1-a2
        L_intra = (Lv1v2 + La1a2)/2

        # total loss
        L_CrissCross = (L_async + L_sync + L_intra)/3

    return L_CrissCross

```

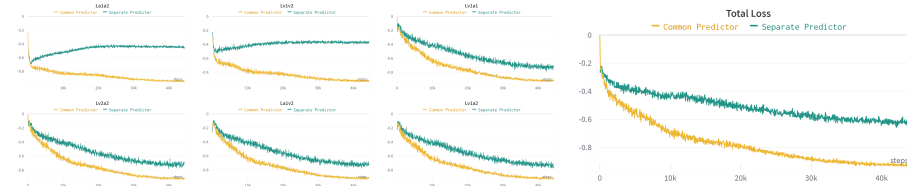


Fig. S2: We present the pretraining loss curves for common vs. separate predictor heads. La1a2 and Lv1v2 refer to the intra-modal losses; La1v1 and La2v2 denote the synchronous cross-modal losses; and finally La1v2 and Lv1a2 refer to the asynchronous cross-modal losses. Note that the minimum possible value for each loss is -1.

S3 Datasets

S3.1 Pretraining Datasets

We use 3 datasets of different sizes for pretraining, namely, Kinetics-Sound [4], Kinetics400 [23], and AudioSet [16]. Kinetics-Sound is a small-scale action recognition dataset, which has a total of 22K video clips, distributed over 32 action classes. Kinetics400 is a medium-scale human action recognition dataset, originally collected from YouTube. It has a total of 240K training samples and 400 action classes. Please note that Kinetics-Sound is a subset of Kinetics400, and consists of action classes which are prominently manifested audibly and visually [4]. Lastly, AudioSet [16] is a large-scale video dataset of audio events consisting of a total of 1.8M audio-video segments originally obtained from YouTube spread over 632 audio classes. Please note that none of the provided labels are used in self-supervised pretraining.

S3.2 Downstream Datasets

Following the standard practices of prior works [41, 40, 2, 3, 5, 27], we evaluate our self-supervised methods on two types of downstream tasks: (i) action recognition based on visual representations and (ii) sound classification based on audio representations. To perform action recognition, we use two popular benchmarks, i.e., UCF101 [58] and HMDB51 [28]. UCF101 consists of a total of 13K clips distributed among 101 action classes, while HMDB contains nearly 7K video clips distributed over 51 action categories. To perform sound classification, we use two popular benchmarks ESC50 [47] and DCASE2014 [59]. ESC50 is a collection of 2K audio events comprised of 50 classes and DCASE2014 is an audio event dataset of 100 recordings spread over 10 categories.

S4 Data Augmentation

Visual Augmentations. The parameters for visual augmentations are presented in Table S1. Some of the parameters are chosen from the literature, while the rest are found through empirical search. We set the parameters of Multi Scale Crop, Gaussian Blur, and Gray Scale as suggested in [11], and the parameters for Color Jitter are taken from [41]. We use TorchVision [44] for all the implementations of visual augmentations, except Cutout where we use the implementation available

Table S1: Visual augmentation parameter details.

Augmentation Parameters	
Multi Scale Crop	<code>min area = 0.08</code>
Horizontal Flip	<code>p = 0.5</code>
	<code>brightness = 0.4</code>
Color Jitter	<code>contrast = 0.4</code>
	<code>saturation = 0.4</code>
	<code>hue = 0.2</code>
Gray Scale	<code>p = 0.2</code>
Gaussian Blur	<code>p = 0.5</code>
Cutout	<code>max size = 20</code> <code>num = 1</code>

Table S3: Visual augmentation summary.

	MSC	HF	CJ	GS	GB	C
Pretraining	✓	✓	✓	✓	✓	✓
Full-finetune	✓	✓	✓	✓	✗	✓
Linear evaluation	✓	✓	✓	✓	✗	✓

here³. Please note that for the Cutout transformation, the mask is created with the mean value of the first frame in the sequence. We summarize the augmentation schemes used for pretraining and evaluation in Table S3.

Audio Augmentations. We present the parameters used for audio augmentations in Table S2. We use the Librosa^[35] library to generate mel-spectrograms. We use the techniques proposed in [43] to perform Time Mask, Frequency Mask, and Time Warp transformations⁴. The parameters for the audio augmentations are set empirically, except for Random Crop which we adopt from [42]. We summarize the augmentation scheme of pretraining and evaluation in Table S4.

S5 Downstream Evaluation Protocol

To evaluate the representations learned with self-supervised pretraining, we test the proposed framework in different setups, namely linear evaluation, full finetuning, and retrieval. The details of the evaluation protocols are mentioned below.

S5.1 Linear Evaluation

To perform linear evaluation of the learned representations on downstream tasks, we extract fixed features (also called frozen features) using the pretrained

³ <https://github.com/uoguelph-mlrg/Cutout>

⁴ <https://github.com/s3prl/s3prl>

Table S2: Audio augmentation parameter details.

Augmentation Parameters	
Volume Jitter	<code>range = ±0.2</code>
Time Mask	<code>max size = 20</code> <code>num = 2</code>
Frequency Mask	<code>max size = 10</code> <code>num = 2</code>
Timewarp	<code>wrap window = 20</code>
Random Crop	<code>range = [0.6,1.5]</code> <code>crop scale = [1.0,1.5]</code>

Table S4: Audio augmentation summary.

	VJ	Mask	RC	TW
Pretraining	✓	✓	✓	✗
Linear evaluation	✓	✓	✓	✓

backbones. We train a linear classifier using the fixed feature representations. The details are presented below.

S5.1.1 Action Recognition.

To perform linear evaluation on action recognition, we follow standard evaluation protocols laid out in prior works [2,50,45,41]. The details are presented below.

HMDB51 and UCF101. We perform linear evaluation in 2 setups, i.e., 8-frame and 32-frame inputs. We evaluate on 8-frame inputs for the design explorations and 32-frame inputs for large-scale experiments.

Following the protocols mentioned in [2,50], we feed 8-frame inputs to the video backbone, with a spatial resolution of 224^2 . During training, we randomly pick 25 clips per sample to extract augmented representations, while during testing, we uniformly select 10 clips per sample and report top-1 accuracy at sample level prediction by averaging clip level predictions. The augmentation techniques are mentioned in Section S4. We don't apply the Gaussian Blur while extracting the training features since it deteriorates the performance. Moreover, to perform a deterministic evaluation, we don't apply any augmentations during validation. The visual features are extracted from the final convolution layer and passed to a max-pool layer with a kernel size of $(1, 4, 4)$ [41]. Finally, we use the learned visual representations to train a linear SVM classifier, we sweep the cost values between $\{0.00001, 0.00005, 0.0001, 0.0005, 0.001, 0.005, 0.01, 1\}$ and report the best accuracy.

When validating on 32-frame inputs, we could not perform SVM as the feature vector is too large to hold in the memory. Hence, we use a linear fully-connected layer at the end of the video backbone. Note that during training the backbone is kept frozen and only the linear layer is trained. we keep the rest of the setup the same as described earlier, with the exception of training where we randomly select 10 clips per sample.

Kinetics400. As Kinetics400 [23] is a large scale dataset, the feature vector is too large to save in memory. Following [41], we use a fully connected layer at the end of the frozen backbone and feed 8×224^2 frame inputs. During training, we randomly pick 1 clip per sample, while during validation, we uniformly select 10 clips per sample. Note that the rest of the setups remain the same, as described for HMDB51 and UCF101. Finally, we obtain the sample level prediction by averaging the clip level predictions and report the top-1 accuracy.

S5.1.2 Sound Classification.

In case of evaluating audio representations, we follow the evaluation protocol laid out in prior works [41,3,2,50] for respective datasets. The details are mentioned below.

ESC50. In case of sound classification on ESC50, we use 2 and 5-second audio inputs to extract audio representations. Following [45], we extract 10 epochs worth of augmented feature vectors from the training clips. During testing, when using 2-second inputs, we extract 10 equally spaced audio segments [41,45,3], and when using 5-second inputs, we extract 1 segment [2,50] from each sample. We perform the augmentations mentioned in Section S4 to extract the training features. We notice that unlike self-supervised pretraining, time warping improves the model

performance in the linear evaluation. We do not apply any augmentations during validation. We extract the representations from the final convolution layer and pass it through a max-pool layer with a kernel size of $(1, 3)$ and a stride of $(1, 2)$ [45]. Similar to action recognition, we perform classification using a one-vs-all linear SVM classifier, we sweep the cost values between $\{0.00001, 0.00005, 0.0001, 0.0005, 0.001, 0.005, 0.01, 1\}$ and report the best accuracy.

DCASE. To validate on DCASE, we follow the protocol mentioned in [41]. We extract 60 clips per sample and train a linear classifier on the extracted representations. Note that the augmentation and feature extraction schemes remain the same as mentioned for ESC50. We report the top-1 sample level accuracies by averaging the clip level predictions.

S5.2 Full Finetuning

Following earlier works [3, 41, 40, 5], we use the pretrained visual backbone along with a newly added fully-connected layer for full finetuning on UCF101 [58] and HMDB51 [28]. We adopt two setups for full finetuning, 8-frame inputs and 32-frame inputs. In both cases we use a spatial resolution of 224^2 . Lastly, we replace the final adaptive average-pooling layer with an adaptive max-pooling layer. We find that applying strong augmentations improves the model performance in full-finetuning. Please see the augmentation details in Section S4. During testing, we extract 10 equally spaced clips from each sample and do not apply any augmentations. We report the top-1 accuracy at sample level prediction by averaging the clip level predictions. We use an SGD optimizer with a multi-step learning rate scheduler to finetune the model. We present the hyperparameters of full-finetuning in Table S10.

S5.3 Retrieval

In addition to full-finetuning, we also perform retrieval to test the quality of the representations in an unsupervised setup. We follow the evaluation protocol laid out in [45, 68]. We uniformly select 10 clips per sample from both training and test splits. We fit 2-second inputs to the backbone to extract representations. We empirically test additional steps such as l2-normalization and applying batch-normalization on the extracted features, and notice that they do not help the performance. Hence, we simply average the features extracted from the test split to query the features of the training split. We compute the cosine distance between the feature vectors of the test clips (query) and the representations of all the training clips (neighbors). We consider a correct prediction if k neighboring clips of a query clip belong to the same class. We calculate accuracies for $k = 1, 5, 20$. We use the NearestNeighbors⁵ API provided in SciKit-Learn in this experiment.

S6 Architecture Details

In this study we use a slightly modified version of R(2+1)D-18 [63] as the video backbone as proposed in [41], and ResNet-18 [21] as the audio backbone. For the sake of completeness we present the architecture details in Tables S5 and

⁵ `sklearn.neighbors.NearestNeighbors`

S6, respectively. The predictor and projector heads are made of fully-connected layers following [12], and their architecture details are presented in Table **S7**.

Table S5: Architecture of the video backbone: R(2+1)D-18.

Layer	X_s	X_t	C	K_s	K_t	S_s	S_t
frames	112	8	3	-	-	-	-
conv1	56	8	64	7	3	2	1
maxpool	28	8	64	3	1	2	1
block2.1.1	28	8	64	3	3	1	1
block2.1.2	28	8	64	3	3	1	1
block2.2.1	28	8	64	3	3	1	1
block2.2.2	28	8	64	3	3	1	1
block3.1.1	14	4	128	3	3	2	2
block3.1.2	14	4	128	3	3	1	1
block3.2.1	14	4	128	3	3	1	1
block3.2.2	14	4	128	3	3	1	1
block4.1.1	7	2	256	3	3	2	2
block4.1.2	7	2	256	3	3	1	1
block4.2.1	7	2	256	3	3	1	1
block4.2.2	7	2	256	3	3	1	1
block5.1.1	4	1	512	3	3	2	2
block5.1.2	4	1	512	3	3	1	1
block5.2.1	4	1	512	3	3	1	1
block5.2.2	4	1	512	3	3	1	1
avg-pool	-	-	512	-	-	-	-

Table S6: Architecture of the audio backbone: ResNet-18.

Layer	X_f	X_t	C	K_s	K_t	S_f	S_t
spectrogram	80	200	1	-	-	-	-
conv1	40	100	64	7	7	2	2
maxpool	20	50	64	3	3	2	2
block2.1.1	20	50	64	3	3	2	2
block2.1.2	20	50	64	3	3	2	2
block2.2.1	20	50	64	3	3	2	2
block2.2.2	20	50	64	3	3	2	2
block3.1.1	10	25	128	3	3	2	2
block3.1.2	10	25	128	3	3	2	2
block3.2.1	10	25	128	3	3	2	2
block3.2.2	10	25	128	3	3	2	2
block4.1.1	5	13	256	3	3	2	2
block4.1.2	5	13	256	3	3	2	2
block4.2.1	5	13	256	3	3	2	2
block4.2.2	5	13	256	3	3	2	2
block5.1.1	3	7	512	3	3	2	2
block5.1.2	3	7	512	3	3	2	2
block5.2.1	3	7	512	3	3	2	2
block5.2.2	3	7	512	3	3	2	2
avg-pool	-	-	512	-	-	-	-

Table S7: Architecture of projector (left) and predictor (right) heads.

Layer Dimensions	Layer Dimensions
input	512
fc-bn-relu	2048
fc-bn-relu	2048
fc-bn	2048
input	2048
fc-bn-relu	512
fc	2048

S7 Hyperparameters and Training Details

In this section, we present the details of the hyperparameters, computation requirements, as well as additional training details of self-supervised pretraining and full finetuning.

S7.1 Pretraining Details

We present the pretraining hyperparameters of CrissCross in Table **S9**. Most of the parameters remain the same across all 3 datasets, with the exception of a few hyperparameters such as learning rates and epoch size which are set depending on the size of the datasets. We train on Kinetics-Sound with a batch size of 512, on a single node with 4 Nvidia RTX-6000 GPUs. Next, when training on Kinetics400 and AudioSet, we use 2 nodes and set the batch size to 2048. Adam [26] optimizer is used to train our proposed framework. We use LARC⁶ [69]

⁶ <https://github.com/NVIDIA/apex/blob/master/apex/parallel/LARC.py>

Table S8: Abbreviations and descriptions of the hyperparameters.

Abbreviations	Name	Description
bs	batch size	The size of a mini-batch.
es	epoch size	The total number of samples per epoch.
ep	total epochs	The total number of epochs.
lr	learning rate	
lr _{ab}	audio backbone lr	
lr _{vb}	video backbone lr	The learning rates to train the networks.
lr _{ap}	audio predictor lr	
lr _{vp}	video predictor lr	
lrs	learning rate scheduler	The learning rate scheduler to train the network.
ms	milestones	At every ms epoch the learning rate is decayed.
γ	lr decay rate	The learning rate is decayed by a factor of γ .
wd	weight decay	The weight decay used in the SGD optimizer.
mtm	momentum	The momentum used in the SGD optimizer.
drp	dropout	The dropout rate.

Table S9: Pretext training parameters. Note the abbreviations used below, KS: Kinetics-Sound, K400: Kinetics400, AS: AudioSet, Adam*: Adam with LARC

dataset	bs	es	ep	optim	lrs	lr _{vb} (start/end)	lr _{ab} (start/end)	lr _{vp}	lr _{ap}	wd	betas
KS	512	220K	100	Adam	Cosine	0.0002/0	0.0002/0	0.002	0.002	0.0001	0.9, 0.999
K400	2048	1M	100	Adam*	Cosine	0.0002/0.0001	0.0002/0.0001	0.002	0.002	0.0001	0.9, 0.999
AS	2048	3.5M	100	Adam*	Cosine	0.0001/0	0.0001/0	0.001	0.001	0.0001	0.9, 0.999

as a wrapper to the Adam optimizer to clip the gradients while pretraining with a batch size of 2048. In this work, we stick to batch sizes of 512 and 2048, because (i) as they show stable performance based on the findings of [12]; (ii) they fit well with our available GPU setups. Additionally, we perform mixed-precision training [36] using PyTorch AMP [44] to reduce the computation overhead.

Ablation Parameters. In the ablation study, we keep the training setup exactly identical across all the variants, with the exception of the learning rates, which we tune to find the best performance for that particular variant. For example, we set the base learning rate for visual-only and audio-only models as 0.0001 and 0.00001 respectively. Next, the predictor learning rates are set to 0.001 and 0.0001 for the visual-only and audio-only variants.

S7.2 Full Finetuning Details

The full finetuning hyperparameters for both the benchmarks are presented in Table S10. We use a batch size of 32 for the 32-frame input and 64 for the 8-frame input. We use an SGD optimizer with multi-step learning rate scheduler to finetune the video backbones. Please note that we perform the full finetuning on a single Nvidia RTX-6000 GPU.

Table S10: Full-finetuning hyperparameters for action recognition when pretrained on Kinetics400.

dataset	input	es	bs	ep	ms	optim	lr	γ	wd	mtm	drp
UCF101	8×224^2	95K	64	20	6/10/14	SGD	multi-step 0.0005	0.3	0.0	0.9	0.0
UCF101	32×224^2	95K	32	20	8/12/16	SGD	multi-step 0.00007	0.3	0.0	0.9	0.0
HMDB51	8×224^2	35K	64	20	6/10/14	SGD	multi-step 0.0005	0.1	0.0	0.9	0.0
HMDB51	32×224^2	35K	32	20	8/12/16	SGD	multi-step 0.0001	0.3	0.0	0.9	0.0

S8 Qualitative Analyses

To perform a qualitative analysis of the learned representations, we visualize the nearest neighborhoods of video-to-video and audio-to-audio retrieval. In this experiment, we use Kinetics400 [23] to pretrain CrissCross. The pretrained backbones are then used to extract training and validation feature vectors from Kinetics-Sound [4]. We use the Kinetics-Sound for retrieval experiment as it consists of action classes which are prominently manifested both audibly and visually. Next, we use the features extracted from the validation split to query the training features. We present the qualitative results in Figures S3 and S4.

S9 Broader Impact

Better self-supervised audio-visual learning can be used for detection of harmful content on the Internet. Additionally, such methods can be used to develop better multimedia systems. Lastly, the notion that relaxed cross-modal temporal synchronicity is useful, can challenge our existing/standard approaches in learning multi-modal representations and result in new directions of inquiry. The authors don't foresee any major negative impacts.



Fig. S3: **Visualization of video-to-video retrieval.** The frames with **black** borders represent the query embedding, and the next 5 frames represent the top-5 neighborhoods. We highlight the correct retrievals with **green**, while the wrong ones are marked with **red**. Additionally, we also mention the class names at the bottom of each frame. We notice very few instances of wrong retrieval, which generally occur when the visual scenes are highly similar, for instance ‘playing piano’ and ‘playing organ’, ‘playing saxophone’ and ‘playing clarinet’.

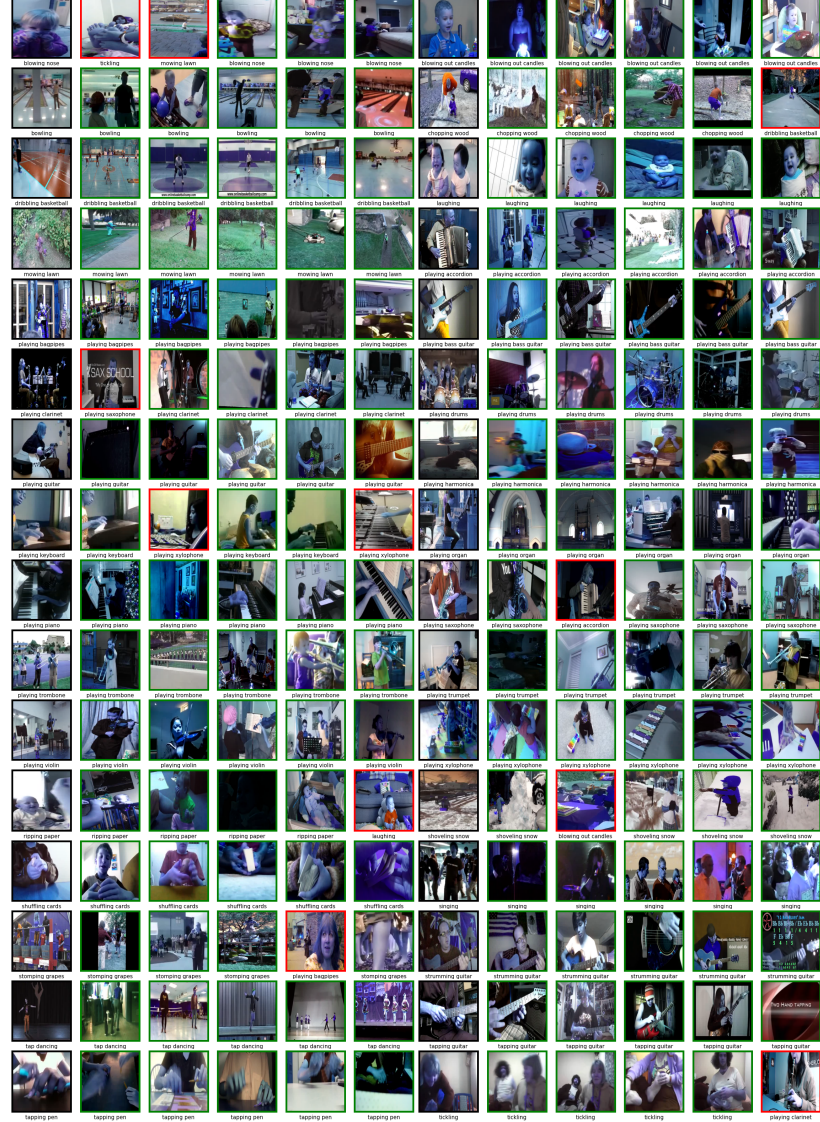


Fig. S4: **Visualization of audio-to-audio retrieval.** The frames with **black** borders represent the query embedding, and the next 5 frames represent the top-5 neighborhoods. We highlight the correct retrievals with **green**, while the wrong ones are marked with **red**. Additionally, we mention the class names at the bottom of each frame. We notice very few instances of wrong retrieval, which generally occur when the sound events are audibly very similar for instance, ‘playing keyboard’ and ‘playing xylophone’, ‘playing saxophone’ and ‘playing accordion’.